Decay Rates of Bound Negative Muons*†

D. D. YOVANOVITCH
The Enrico Fermi Institute for Nuclear Studies, The University of Chicago, Chicago, Illinois
(Received September 24, 1959)

The decay rate of negative muons bound to nuclei of atomic number Z, $\Lambda_d(Z)$, has been investigated experimentally by two independent methods: (a) the "sandwich" method, and (b) the "calibrated efficiency" method. Both methods are based on the fact that the negatron yield per muon, $y^-(Z)$, is proportional to $\Lambda_d(Z)/\Lambda_t(Z)$, where $\Lambda_t(Z)$ is the total disappearance rate of negative muons for element Z, and are designed to avoid absolute measurements of $y^-(Z)$. In method (a), μ^- are stopped in a multilayer "sandwich" target made by alternately stacking sheets of two elements Z, Z', and the resultant e^- time distribution is decomposed into components due to Z and Z'. The ratio of muon stops in Z and Z' is established *empirically;* knowing $\Lambda_d(Z')$, $\Lambda_d(Z)$ can be computed. This method was applied to Al, Fe, Zn, Cd, Mo, W, and Pb. In method (b), μ^- and μ^+ of *identical* range distributions are stopped in a given target, and the e^+ yield, y^+, is used as a calibration of the e^- counting efficiency. This method has been applied to C, Ca, Ti, V, Mn, Fe, Co, Ni, Zn, I, and Pb. The sources of error of either method are discussed in detail. The results indicate:

(1) In the range $20<Z<30$, $\Lambda_d(Z)>\Lambda_d(0)$, i.e., the bound decay rate exceeds the vacuum (i.e., μ^+) decay rate; $\Lambda_d(Z)$ presents a sharp peak near $Z=26$.

(2) For $Z>30$, one finds $\Lambda_d(Z)<\Lambda_d(0)$, i.e., the decay is *inhibited* by binding. The effect is very marked for the heaviest elements, e.g., $\Lambda_d(82)/\Lambda_d(0)=0.34\pm0.04$.

These results are compared with the predictions of simplified theoretical models. The peak near $Z=26$ is tentatively attributed to the Coulomb enhancement of the outgoing electron wave function at the point of decay.

I. INTRODUCTION

THE general behavior of negative muons in matter is well understood in terms of the picture in which the muons rapidly reach the ground states of the mesic atoms, and disappear from these states by the competing processes of capture and of decay. The capture rates will depend strongly on the Z, the atomic number of the capturing nucleus, because the probability of finding the muon inside nuclear matter is strongly Z-dependent. This Z-dependence, first quantitatively discussed by Wheeler,[1] has by now been well investigated in this laboratory[2] and elsewhere.[3] The decay rates, on the other hand, should in some first approximation not be affected at all by the fact that the muons are bound, inasmuch as the decay process is a purely leptonic one. There are, however, several obvious physical effects which will bring about finite differences between the bound decay rates and the vacuum decay rate (which may be taken as that of a positive muon), and some of these have been the subject of theoretical investigations[4–7]:

(a) the decay rate is proportional to the fifth power of the available energy, and this quantity differs for a bound muon from the muon rest mass;

(b) the orbital motion leads to a Doppler smearing of the decay spectrum as well as to a time dilation;

(c) the outgoing election can no longer be described by a plane wave, being strongly attracted to the point of decay by the nuclear Coulomb potential.

Experimentally, the decay of bound muons has so far been investigated in much less detail than the capture process.[8,9] The purpose of the present work is to provide empirical evidence for the effects just mentioned through the measurement of the decay rates of negative muons bound to various nuclei throughout the periodic table. Inasmuch as none of the theoretical calculations performed to date can claim more than semiquantitative validity [effect (c) having been neglected and the finite size of the nucleus not having been properly taken into account], the results of the present investigation may be useful for several reasons:

(1) The calculation of precise muon-capture rates from the experimentally accessible muon disappearance rates requires the knowledge of the decay rates.[2]

(2) The experimental determination of the relative *atomic* capture probabilities of the constituents of chemical compounds in which muons are brought to rest, if performed by the convenient method of studying the time dependence of the electron appearance rates,[10] also requires a knowledge of the bound decay rates for the mesic atoms in question.

(3) The determination of muon-capture rates from the number of decay electrons per muon, such as performed by Lederman and Weinrich,[11] becomes quantitatively meaningful only once the specific bound decay rates are known or can at least be interpolated from data on neighboring nuclei.

Section II of this paper contains a description of the experimental procedures used in our measurements.

* Research supported by a joint program of the Office of Naval Research and the U. S. Atomic Energy Commission.

† A thesis submitted to the Department of Physics, the University of Chicago, in partial fulfillment of the requirements for the Ph.D. degree.

[1] J. A. Wheeler, Revs. Modern Phys. **21**, 133 (1949).

[2] J. C. Sens, Phys. Rev. **113**, 679 (1959).

[3] For a survey, see J. Rainwater, *Annual Review of Nuclear Science* (Annual Reviews, Inc., Palo Alto, 1957), Vol. 7, p. 1.

[4] C. E. Porter and H. Primakoff, Phys. Rev. **83**, 849 (1951).

[5] T. Muto *et al.*, Progr. Theoret. Phys. (Kyoto) **8**, 13 (1952).

[6] N. D. Khuri and A. S. Wightman (private communication).

[7] H. Primakoff (private communication).

[8] F. E. Holmstrom and J. E. Keuffel (unpublished).

[9] A. Astbury *et al.*, Proc. Phys. Soc. (London) **73**, 314 (1959).

[10] J. C. Sens *et al.*, Nuovo cimento **7**, 314 (1959).

[11] L. Lederman and M. Weinrich, *Proceedings of the CERN Symposium on High-Energy Accelerators and Pion Physics, Geneva, 1956* (European Organization of Nuclear Research, Geneva, 1956), Vol. 2, p. 427.

The various sources of error and the corrections applied in deriving the final decay rates are discussed in Sec. III, while Sec. IV is devoted to the discussion of the results.

II. EXPERIMENTAL PROCEDURE

A. Description of Methods

Negative muons stopped in an elemental target of atomic number Z disappear at a rate[12]

$$\Lambda_t(Z)=\Lambda_d(Z)+\Lambda_c(Z), \tag{1}$$

where $\Lambda_d(Z)$ is the decay rate and $\Lambda_c(Z)$ the capture rate specific to the target Z in question.[13] If N_μ^- negative muons are stopped at $t=0$, the decay electrons will appear at a rate

$$dN_e^-/dt=\Lambda_d(Z)N_\mu^-\exp[-\Lambda_t(Z)t], \tag{2}$$

i.e., with a time dependence characterized by $\Lambda_t(Z)$. The total electron yield per stopped muon, Y_e^-, is given by

$$Y_e^-=N_e^-/N_\mu^-=\Lambda_d(Z)/\Lambda_t(Z), \tag{3}$$

and is a measure of the desired quantity $\Lambda_d(Z)$, once $\Lambda_t(Z)$ is known, say from the study of Eq. (2). In practice, the decay electrons from a finite target Z will be detected with an efficiency $\epsilon^-(Z)$ and a solid angle $\Delta\Omega^-(Z)$ with an actual yield $y^-(Z)$:

$$y^-(Z)=\Delta\Omega^-(Z)\epsilon^-(Z)\Lambda_d(Z)/\Lambda_t(Z). \tag{3'}$$

The determination of the product $\Delta\Omega^-(Z)\epsilon^-(Z)$, i.e., the absolute counting of electrons, necessary for a measurement of $\Lambda_d(Z)$ poses considerable problems. To circumvent these, we have adopted two independent methods:

(*a*) *"Sandwich" method.* Here one compares the electron yields $y^-(Z)$ and $y^-(Z')$ from two constituents Z, Z' of multi-layer target compounded of alternate sheets of two elements Z and Z'. The separation of the observed electron yield into $y^-(Z)$ and $y^-(Z')$ is done by decomposing the observed time distribution into two components characterized by $\Lambda_t(Z)$ and $\Lambda_t(Z')$, respectively. One has

$$\frac{y^-(Z)}{y^-(Z')}=\frac{\Delta\Omega^-(Z)\epsilon^-(Z)}{\Delta\Omega^-(Z')\epsilon^-(Z')}\frac{\Lambda_d(Z)}{\Lambda_d(Z')}\frac{\Lambda_t(Z')}{\Lambda_t(Z)}. \tag{4}$$

The "sandwich" arrangement allows one to take (except for minor effects which will be discussed in detail later) the first quotient equal to unity. Thus $\Lambda_d(Z)$ can be determined if $\Lambda_d(Z')$ is known [the quantity $\Lambda_t(Z)/\Lambda_t(Z')$ is readily available, e.g., from the observed time distribution]. Taking Z' sufficiently small, one may assume $\Lambda_d(Z')\approx\Lambda_d(0)=\Lambda_d^+$, the decay constant of the positive muon. With this assumption, the "sandwich" method gives $\Lambda_d(Z)$ as

$$\Lambda_d(Z)=\frac{y^-(Z)\Lambda_t(Z)}{y^-(Z')\Lambda_t(Z')}\Lambda_d(0)=R(Z)\Lambda_d(0), \tag{5}$$

the quantity $R(Z)$ characteristic of the departure of the decay rate of a muon bound to a nucleus Z from the vacuum decay rate $\Lambda_d(0)$, being defined by Eq. (5). To evaluate Eq. (5), one must of course accurately know the ratio of muon stops $N_\mu^-(Z)/N_\mu^-(Z')$. This quantity could in principle be calculated from known stopping power data, but it is much more reliable to determine it by direct measurements.

(*b*) *"Calibrated efficiency" method.* Here μ^- and μ^+ mesons of identical range distributions are stopped in the same target Z, and the yields $y^-(Z)$, $y^+(Z)$ of negative and positive electrons are determined in the same counting geometry. Denoting by an index $+$ the quantities pertaining to positron counting, one has

$$\frac{y^-(Z)}{y^+(Z)}=\left(\frac{\Delta\Omega^-(Z)\epsilon^-(Z)}{\Delta\Omega^+(Z)\epsilon^+(Z)}\right)\frac{\Lambda_d(Z)}{\Lambda_d(0)}\frac{\Lambda_d(0)}{\Lambda_t(Z)}. \tag{6}$$

Assuming that the positive and negative electrons in question have identical range properties, the "efficiency" quotient in Eq. (6) may be set equal to unity, and one may write

$$\Lambda_d(Z)=R(Z)\Lambda_d(0)=\Lambda_t(Z)y^-(Z)/y^+(Z). \tag{6'}$$

Method (a) has certain advantages over method (b), but is limited by the fact that not all elemental targets are available in sheet form. In both methods the ultimate limitation on the accuracy with which $R(Z)$ can be determined is set by the uncertainties in the disappearance rates $\Lambda_t(Z)$.

There are two effects which have to be considered in using either of these two methods to determine $\Lambda_d(Z)$:

(1) In determining the yields $y^-(Z)$ one must make sure that one is effectively counting electrons and not γ rays. Since about two or three γ rays are produced per μ^- capture[2] (presumably in the de-excitation of the capture products) and since the ratio $\Lambda_c/\Lambda_d\gtrsim 10$ for the Z's of interest, even a small sensitivity of the "electron" detector to γ's can cause a large error in $R(Z)$. In a heavy element like Pb for instance, where the number of capture γ's is about 100 times larger than the number of decay electrons, a 1% efficiency of counting γ's would cause a systematic error of about 100% in $R(Z)$. The electron telescope used in the present experiment was so designed as to have an efficiency of $<0.1\%$ for counting γ's of energies below 10 Mev.

(2) The μ^- and μ^+ beams used in the measurements may be highly polarized (viz., 70% in the case of the Chicago 145 Mev/c beams[14]) and thus yield anisotropic electron distributions when brought to rest in not completely depolarizing media. In comparing the electron

[12] We assume though that solely muon decay contributes to the electron yield, i.e., that the process $N+\mu^-\rightarrow N+e^-$ never takes place. Empirically, one knows only that this is 5×10^{-4} rarer than muon decay for $Z=29$ [see: J. Steinberger and H. B. Wolfe, Phys. Rev. **100**, 1490 (1957)].

[13] We neglect any dependence of Λ_d and Λ_c on quantities other than Z, e.g., on A.

[14] R. A. Swanson, Phys. Rev. **112**, 580 (1958).

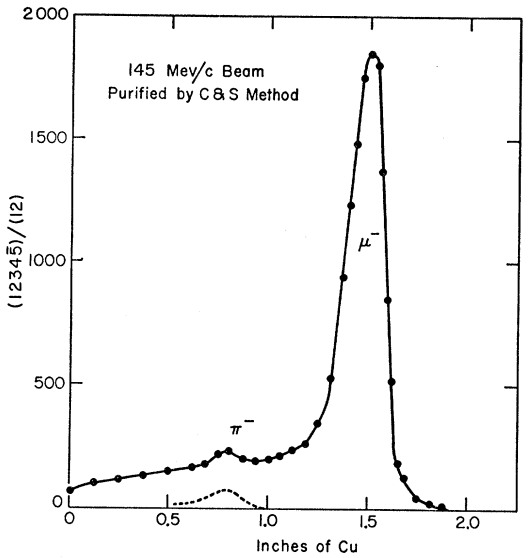

FIG. 1. Differential range curve of the 145 Mev/c negative "muon" beam used. Beam is purified by the method of Campbell and Swanson.[16]

yields from different targets (or from muons of opposite sign in a given target) in a fixed direction, one has to take the dependence of the asymmetry on the type of the target and the sign of the muons duly into account. Thus positive muons appear to retain their full polarization in conductors,[14] while negative muons reaching the K shell appear to retain in the most favorable cases (targets with spin zero nuclei) no more than about 20% polarization.[15] This circumstance would falsify the results obtained by method (b) by a factor $f=(1-\bar{a}^+)/(1-\bar{a}^-)$, where $\bar{a}^\pm$ indicates the effective asymmetry parameters for the two muon charges in the characteristic distribution $W(\theta)=1+\bar{a}^\pm\cos\theta$ (θ=angle between μ-beam and electron emission directions). The error introduced by the same effect in method (a) would however be much smaller, since one compares these two yields from negative muons, and $\bar{a}^-$ is known not to exceed 0.04 in absolute magnitude.[15] As will be discussed below, it is possible to eliminate these asymmetry effects by the use of suitable magnetic field arrangements.

B. Experimental Arrangements

1. Beam Characteristics

The purity of the "muon" beams used and the precise knowledge of their range distributions is very important in either of the two methods described above. The negative beam had to meet the following requirements:

(a) be free of e^- contamination—electrons stopping in the target would introduce spurious "muon" counts;

(b) have a minimal π^- contamination—the pion-star products could also effect the muon counting (see below).

We used a purified beam prepared by the method of Campbell and Swanson.[16] The range distribution of this beam, of about 82-Mev mean muon energy, is shown on Fig. 1. This figure shows clearly that both requirements (a) and (b) were well met. The flux of this beam, measured in terms of μ^- stops in a target of 6–8 g/cm^2 thickness, was 1–1.2 μ^-/cm^2 sec over a target area of about 10^2 cm^2.

The positive beam, used in method (b), did not have to be purified as extensively as the negative one, possessing inherently[14] a smaller electron contamination. On the other hand, by the very nature of the "calibrated efficiency" method, the mean range and the range distribution of the positive muons had to match these same features of the negative muon beam as closely as possible. Figure 2 shows a comparison of the μ^- and μ^+ range distributions as determined near the peaks of these distributions with Cu absorbers. In order to insure the reproducibility of these distributions for all targets, we monitored the magnetic field of the steering magnet used for the momentum analysis of the incident beam with a Li nuclear resonance probe.[17] With this precaution, the reproducibility in locating the centroids of the range distributions was in all runs better than ± 0.05 g/cm^2 of moderator.

2. Counter Layout and Electronics

The counter arrangements used in both methods were sufficiently similar so as not to require separate

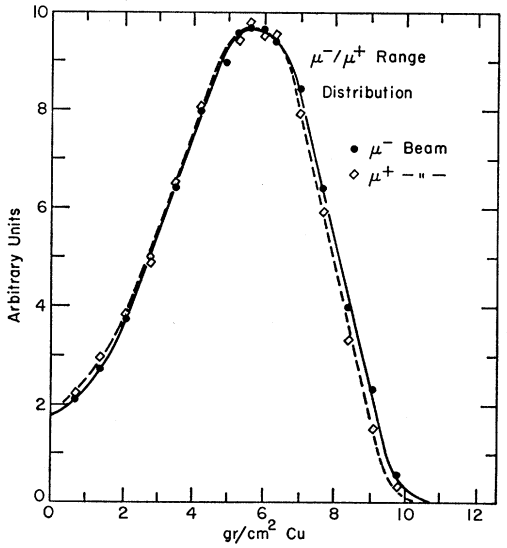

FIG. 2. Differential range curves of μ^-/μ^+ beams used: compared near the end of their range.

[15] A. E. Ignatenko *et al.*, J. Exptl. Theoret. Phys. U.S.S.R. **35**, 1131 (1958) [translation: Soviet Phys. JETP **35**(8), 792 (1959)].

[16] N. P. Campbell and R. A. Swanson (unpublished report).

[17] Preliminary experiments had indicated that the variation of the fields (1–2%) upon reversal of the current through the steering magnet (due to hysteresis of the latter) has a very drastic effect on the range distribution. The beam composition was also found to be very strongly affected by even slight radial displacements of the cyclotron target.

description. The general layout will be described with reference to Fig. 3, indicating later, whenever necessary, the slight modifications that were made when switching from one method to the other.

All counters, 1 through 7, consisted of square plastic scintillators coupled by Lucite light pipes to 6810-A photomultipliers. The "muon" beam, incident on counter 1, passed through a lead collimator Pb and then through a copper moderator Cu of sufficient thickness ($\sim$28 g/cm^2) to center the muon range curve in the target T (6–10 g/cm^2). A muon stopping in T was signalled by the coincidence-anticoincidence combination (12345) ("μ-telescope"). Especially with the negative beam, the two counters (3 and 4) behind the Cu moderator were essential in reducing the number of spurious muon counts due to the pion induced short range particles (protons and neutrons)[2]. In the "sandwich" runs counter 4 consisted of a thin ($\frac{1}{16}$ in.) scintillator 4×4 in. in area, this choice was essential for measuring the number of stops in the various layers of the "sandwich" targets.

The coincidence part of the electron telescope consisted of one $\frac{1}{4}$-in. thick scintillator 5.5×5.5 in. in area (counter 5) and of two $\frac{1}{8}$-in. scintillators 8×8 in. in area (counters 6 and 7), with two of $\frac{5}{16}$-in. thick Al sheets sandwiched between them. In method (a) the same counters were of smaller area (6×6 in.), but the other features of the telescope were unchanged. An electron originating from the target was signalled by the combination (4567) ("e-telescope"), where the 4 anticoincidence excluded electrons coming from decays in the moderator. This anticoincidence requirement suppressed also all true electron events within about 10 mμsec from $t=0$ (the arrival time of the muon), a fact which leads to corrections which will be discussed later.

The total mass of the (567) electron telescope, including the Al absorber, was 5.5 g/cm^2. To get an upper limit to its γ-ray sensitivity, we may first consider this combination as (57) doubles telescope; according to the data of Bleuler and Zunti,[18] such a combination (with the amount of absorber just specified) would have an efficiency $<10^{-3}$ for a single photon of 10 Mev (and less for softer radiations). In view of the fact that probably several nuclear de-excitation γ's are emitted simultaneously after muon capture, the actual sensitivity of such a doubles telescope could however be slightly higher than 10^{-3}, through the occurrence of two simultaneous Compton events. The triples combination (567) actually used here eliminates such events completely, while the probability of analogous threefold events is negligibly small. The effectiveness of the addition of a third counter was borne out by auxiliary measurement in which μ^- and μ^+ decays in Cu were compared.

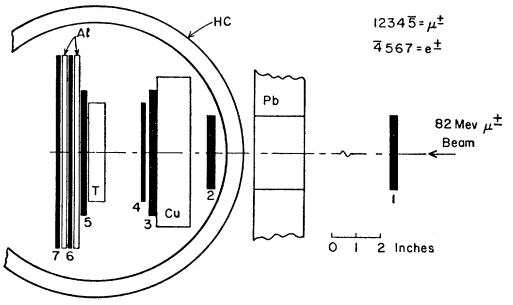

FIG. 3. Experimental arrangement for the measurement of the decay rates.

Both the (12345)-"stop" and (4567)-"start" signals were generated by Garwin type[19] coincidence circuits followed by fast triggers.[20] These "start" and "stop" signals were fed to a time-to-pulse-height converter (T.C.) as timing pulses, in a manner already described in detail elsewhere.[2,14] The T.C. output was fed to a 100-channel pulse-height analyzer (PHA).

The output rates of both (e and μ) telescopes were monitored by 10 Mc/sec scalers (H.P. 520 A), followed by conventional slow decades. In determining the yields $y^{\pm}$, the relevant number of muons is that of those capable of contributing an "analyzable" electron. In view of the finite dead-time of the T.C.-PHA combination used here (400 μsec per analysis, leading to about 20–30% loss for the beam rates used), this number was substantially different from the essentially loss-free output of the μ-telescope scaler. To correct for this, the μ-telescope output was monitored through a simple transistor block gate which received its block signal from PHA, thus preventing the counting of any muon arriving during an analysis.[21]

A pair of Helmholtz coils, indicated as HC in Fig. 3, was mounted together with the counters to provide the compensating and/or precessing fields required in the various parts of the experiment. The axes of these coils were centered with respect to the target T.

3. *Muon Stop Distribution in "Sandwich" Targets*

The ratio of μ stops in the two constituents Z, Z' of each "sandwich" target was measured as follows:

Contrary to what is indicated on Fig. 3, counter 4 ($\frac{1}{16}$ in. thick) was moved quite close to counter 5, so as to leave only a gap of the width of target sheet between these two counters. The number, n_1, of muons (per fixed monitor) that stopped in 4 with the correct amount of moderator in place was first measured as (12345) with the target out (i.e., with nothing between counters 3 and 4). Next, the first sheet of the "sandwich," of element Z, was inserted between 4 and 5; this gave N_1

[18] E. Bleuler and W. Zünti, Helv. Phys. Acta **19**, 77 (1946); see also W. A. Fowler, C. C. Lauritsen, and T. Lauritsen, Revs. Modern Phys. **20**, 236 (1948).

[19] R. L. Garwin, Rev. Sci. Instr. **24**, 618 (1953).

[20] W. C. Davidon and R. B. Frank, Rev. Sci. Instr. **27**, 15 (1956).

[21] We are indebted to R. A. Swanson for pointing out this effect and for the design of the gate circuit.

TABLE I. "Sandwich" compositions.

Z/Z' (1)	"Sandwich" (2)	Number of sheets (3)	Thickness[a] in cm of single sheets Z (4)	Z' (5)	$N_\mu^-(Z)=\Sigma(N_i-n_i)$ (6)	$N_\mu^-(Z')=\Sigma(M_i-m_i)$ (7)	S (8)
13/6	Al-CH_2	2×12	0.163	0.076	9550	5180	1.84±0.05
26/6	Fe-CH_2	2×10	0.061	0.038	23 178	5053	4.59±0.10
30/6	Zn-CH_2	2×8	0.155	0.038	42 260	5740	7.36±0.20
42/13	Mo-Al	2×8	0.101	0.163	16 362	7682	2.13±0.05
48/6	Cd-CH_2	2×8	0.165	0.038	45 220	5468	8.27±0.20
74/6	W-CH_2	2×6	0.050	0.038	31 420	5480	5.72±0.20
82/26	Pb-Fe_I[b]	2×6	0.160	0.061	21 356	7036	3.03±0.10
82/26	Pb-Fe_{II}[b]	2×6	0.160	0.035	19 103	4557	4.19±0.12

[a] All sheets 10×10 cm in area.
[b] Two Pb-Fe "sandwich" targets differing in thickness of Fe sheets.

counts per monitor, corresponding to stops in 4 and in the target sheet Z in question. (N_1-n_1) gives hence the number of stops in this sheet. This same sheet was then transferred into the target position (between 3 and 4), and another measurement taken, giving m_1 stops per monitor. Hereafter the second sheet of the "sandwich," made of element Z', was inserted between 4 and 5, yielding M_1 stops per monitor. The number (M_1-m_1) represents the stops in sheet Z'. Proceeding in the same manner, the whole "sandwich" was stacked, taking for each sheet two counts: once inserting it between 4 and 5, and once adding it to the already measured sheets between 3 and 4. The sum $\sum(N_i-n_i)$ is the number of muons stopping in the component Z, and the sum $\sum(M_i-m_i)$ is the corresponding number for the component Z'. The quantity of interest is the ratio $S=\sum(N_i-n_i)/\sum(M_i-m_i)$ of muon stops, i.e., $S=N_\mu^-(Z)/N_\mu^-(Z')$ [compare the remarks after Eq. (5)]. Concerning the geometry of these measurements, it is worth pointing out that the anticoincidence counter 5 was considerably larger in area (5.5×5.5 in.) than the "sandwich" sheets (3×3 in.), and that the over-all thickness of the "sandwich" targets never exceeded $\frac{3}{4}$ in. so that the relative change in solid angle during the process of stacking was negligible.

III. DATA ANALYSIS

A. Sandwich Method Data

The elements Al, Fe, Zn, Cd, Mo, W, and Pb were investigated by the "sandwich" method; a preliminary account of the results, not including the Pb data, has already been given.[22] In general, the targets consisted of 6 to 12 sheets of the element in question, interspersed with an equal number of "carbon" (polyethylene, CH_2) sheets. The total mass (and hence the individual thicknesses) of the latter was so chosen that the heavy and the light components of each sandwich contributed roughly equal numbers of decay electrons. For the Mo (Pb) measurements, Al (Fe) was used instead of "carbon" as the light component of the sandwich in order to optimize the ratio of the target thickness to the total number of sheets. In typical runs, about 10^4 electrons were collected from each component of a sandwich. For the heaviest elements, W and Pb, this number was limited to about 3×10^3 in view of the particularly low electron yields.

The time distribution of the decay electrons, as displayed on the P.H.A., is readily resolved on a logarithmic plot into two components characterized by the disappearance rates $\Lambda_t(Z)$ and $\Lambda_t(Z')$. This is illustrated in Fig. 4, which is a typical plot obtained with a Fe-CH_2 target. The electron yield $y^-(Z)$ contributed by element Z is essentially given (i.e., except for normalization to the number of pertinent muon stops) by the area under the component of slope $\Lambda_t(Z)$. Indicating the ordinate of the electron rates at $t=0$ by $N_0(Z)$ one has

$$y_e^-(Z)\sim N_0(Z)/\Lambda_t(Z). \quad (7)$$

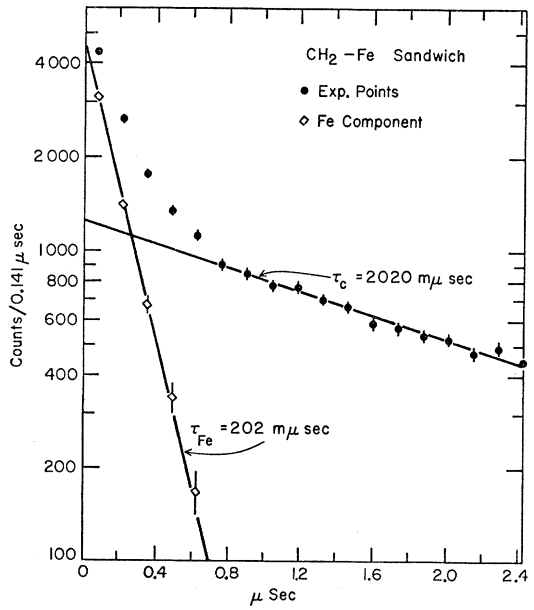

FIG. 4. Time distribution of the decay electrons from Fe-CH_2 "sandwich" target. Indicated lifetimes correspond to $\Lambda_t^{-1}(6)$ and $\Lambda_t^{-1}(26)$ for the two elemental components of the "sandwich." The indicated errors represent statistical standard deviations.

[22] R. A. Lundy *et al.*, Phys. Rev. Letters **1**, 102 (1958).

TABLE II. "Sandwich" method data.

Z/Z' (1)	"Sandwich" (2)	$\Lambda_t(Z)$ (3)	$\Lambda_t(Z')$ (4)	Analyzed electrons (5)	S (6)	$N_0(Z)/N_0(Z')$[a] (7)	$R(Z)$ (8)
13/6	Al-CH_2	11.3±0.3	4.90±0.4	41 719	1.84±0.05	1.82±0.05	0.99±0.04
26/6	Fe-CH_2	49.7±0.7	4.90±0.4	26 570	4.59±0.10	5.57±0.14	1.21±0.05
30/6	Zn-CH_2	62.1±1.0	4.90±0.4	9839	7.36±0.20	7.09±0.20	0.96±0.05
42/13	Mo-Al	95.2±1.8	11.3 ±0.10	8329	2.13±0.05	1.98±0.06	0.93±0.05
48/6	Cd-CH_2	104.5±4.0	4.90±0.04	10 799	8.27±0.20	7.42±0.30	0.90±0.05
74/6	W-CH_2	123.5±3.0	4.90±0.04	7333	5.72±0.20	3.03±0.10	0.53±0.05
82/26	Pb-Fe_I	121.9±4.0	49.7 ±0.7	5309	3.03±0.10	0.66±0.04	0.27±0.10[b]
82/26	Pb-Fe_{II}	121.9±4.0	49.7 ±0.7	9684	4.19±0.12	0.98±0.05	0.28±0.10[b]

[a] Asymmetry correction, f_a, included (see text).
[b] Corrected by $R(26)=1.21$.

It is therefore essential that the position of the $t=0$ axis be accurately known. Experimentally, this position is determined by letting the direct beam traverse both telescopes (i.e., by removing all anticoincidence requirements) and by observing on the P.H.A. the channel number corresponding to the simultaneous events so produced. The position of the time zero channel could in this way be determined with an accuracy of ±10 mμsec. The drift of this position during the entire experiment did not exceed this amount.

The range covered by the T.C. was so chosen as to give a clear display of the short component. Thus this range was ~6 μsec for the Al-CH_2 combination, ~3 μsec for the Fe-CH_2 sandwich, and ~1 μsec for all the other targets. The P.H.A. data were lumped into groups of 5 channels, starting with that channel nearest to $t=0$ which was not affected by the anticoincidence action of $\overline{4}$.

The resultant data were least-squares fitted, with the help of an electronic computer (IBM 650), to a time distribution of the form $f(t)=A\exp[-\Lambda_t(Z)t]+A'\exp[-\Lambda_t(Z')t]+B$.[23] A, A' and the background B were the unknown parameters, while the total disappearance rates $\Lambda_t(Z)$ and $\Lambda_t(Z')$ were available from other work.[2] The values of A and A' so obtained were then corrected for the true position of time zero, and for finite channel width effects. The corrected parameters, when divided by the fraction of muons stopping in the pertinent component, give directly the required yields y^- to be used in Eq. (5), when the light sandwich component is "carbon" or Al. Where Fe was used as the light component, the yield y^-(Fe) is corrected by the $R(Z)$ value for Fe already determined previously.

A summary of the constitution of the sandwich targets is given in Table I, while the data obtained with these targets are summarized in Table II.

B. Calibrated Efficiency Method Data

The elements C, Ca, Ti, V, Mn, Fe, Co, Ni, Zn, I, and Pb were investigated by this method. This selection of targets was made with a twofold purpose: (a) to investigate closely the region $20\leq Z\leq 30$, and (b) to check the $\Lambda_d(Z)$ values obtained for certain elements, in particular Pb, by the sandwich method by an independent measurement. All $Z\leq 30$ except carbon had about equal thicknesses in radiation lengths, viz., about $0.55x_0$ (this corresponds to 1 cm of Fe). This choice was made in order to make the comparison of the electron yields from targets in this group particularly easy and reliable. In view of the target thickness required to stop muons efficiently (6 to 8 g/cm²), the same requirement would have been impractical for C, I, and Pb. All targets were 10 cm×10 cm in area, and were supported by thin styrofoam frames. The latter insured reproducible positioning with respect to the counters.

Typical average rates in this part of the experiment were 130 μ^+ stops/sec and 30 e^+/sec with the positive beam. The negative beam gave about 120 μ^- stops sec, while the electron rate varied from 20 e^-/sec (for C) down to 0.2 e^-/sec (for Pb). We aimed at collecting 10^4 e^- and 3×10^4 e^+ per target; for the e^- from the heaviest targets this goal could again not be attained in view of their low yields. The statistical error contributed by the electron counts was however for all targets smaller than other experimental uncertainties which will be discussed below.

Figure 5 shows the time distributions of positive and negative electrons obtained with a Zn target. The number of stopped muons contributing to either distribution is indicated in the figure. The background observed in the μ^- runs came from two sources: (a) accidentals from uncorrelated $\mu-e$ events, and (b) "carbon" background due to μ^- stops in the counter wrappings, and in the carbon and other light impurities contained in the targets themselves. Source (b) contributed about ten times as much as source (a). In all cases the ratio, β, of the electron counts due to true events and to background, taken at time zero, was 20 or better.

The data were analyzed by first subtracting the extrapolated background from the total number of counts in a given time distribution. The resultant number was further corrected for (1) anticoincidence loss near $t=0$, (2) possible asymmetry effects, and

[23] In this analysis we neglected the factor $\exp(Mt)$, where M = instantaneous stop rate, which would in principle multiply $f(t)$ (see, e.g., discussion in references 2 and 14). This was justified by the smallness of the stop rates used: $M=8\times10^3$.

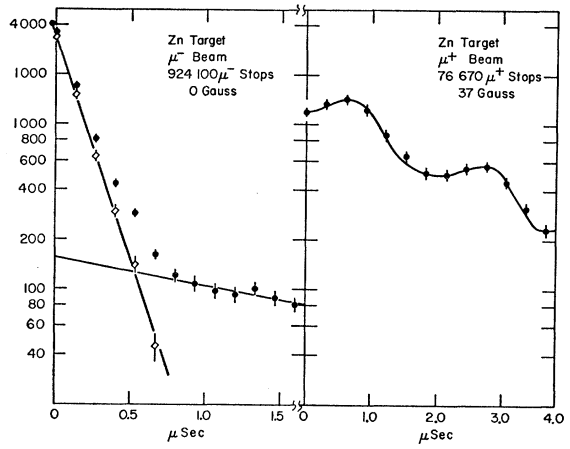

FIG. 5. Time distributions of e^- and e^+ from Zn target. The indicated errors represent statistical standard deviations. The background in e^- time-distribution is due to "carbon" contamination.

(3) differences between the e^+ and e^- energy spectra from a given target.

Our measurements by the calibrated efficiency method are summarized in Table III. This table contains all the relevant information to justify the errors in $R(Z)$ quoted in its last column.

C. Corrections and Errors

We shall first list here errors which could readily be eliminated or corrected for, and then discuss one important systematic uncertainty—the possible difference between e^+ and e^- spectra—for which we had to make an allowance in the error quoted for $R(Z)$ without being able to assess its magnitude quantitatively. It is perhaps worth pointing out that the sources of errors discussed here play an equally important role when a principle similar to that of "calibrated efficiency" method is used to measure muon *capture rates* as was the case in the work of Lederman and Weinrich.[11]

1. Muon Distribution within the Target

The electron yield from a given target is a strong function of the range distribution of muons which stop in it. Experimentally, we found that for the medium Z targets, such as Fe, a displacement of the centroid of the muon range peak by $\frac{1}{32}$ in. within the target produced a 10% change in the electron yield. In order to equalize the corresponding e^+ and e^- counting efficiencies to within better than $\pm 1\%$, one has hence to position μ^+ and μ^- range distributions within a target to an accuracy of 0.1 g/cm² of the moderator. In the present experiment the accuracy of this exceeded 0.05 g/cm². As already mentioned, monitoring the analyzer magnet field with a Li resonance probe insured reproducibility to the same accuracy.

2. Asymmetries in the $e^\pm$ Angular Distributions

As a consequence of well-known effects, the time distribution of positive and negative electrons emitted along the beam direction may be modulated as $P(t) = e^{-\Lambda_t t}(1-\bar{a}\cos\omega t)$, if the muons retain some polarization when brought to rest in a target that is placed in an external magnetic field B. The total number of electrons is given by:

$$N_e^- = \int_0^\infty (1-\bar{a}\cos\omega t)\exp(-\Lambda_t t)dt = [1-\bar{a}x^2/(1-x^2)]/\Lambda_t \quad (8)$$

where $\omega/2\pi = eB/mc = 13.5$ kc/gauss and $x=\Lambda_t/\omega$. The term in square brackets represents a correction which depends on B and on the asymmetry coefficient $\bar{a}$.

The μ^+ runs were performed in the field $B=35$ gauss, where $x=0.15$ with coefficients $\bar{a}$ of about -0.22 for most of the targets (the ferromagnetic elements Fe, Co, Ni, and also I, depolarize μ^+'s) resulting in a correction of less than 0.1%. The μ^- runs were made with the external field B compensated to zero, because the high magnetic fields necessary to make x small appeared

TABLE III. "Calibrated efficiency" data.

Z		Disapp. rate $A_s(Z)$ $\times 10^5$ sec^{-1} (1)	Anal. electr. (2)	β (3)	$f_{a\text{-}e}$ (4)	f_a (5)	y_e^- uncorr. $\times 10^{-3}$ (6)	y_e^- [a] corr. $\times 10^{-3}$ (7)	y_e^+ [b] $\times 10^{-3}$ (8)	$R(Z)$ (9)
6	C	4.90±0.04	27 709	35	1.011±0.005	1.04±0.01	127 ±2	127 ±2	141±1	1.00±0.02
20	Ca	30.0 ±0.3	9117	21	1.067±0.007	1.04±0.01	19.9 ±0.3	21.1 ±0.5	142±1	1.00±0.03
22	Ti	30.3 ±0.5	9687	66	1.068±0.010	1.00±0.01	20.2 ±0.3	21.4 ±0.5	143±1	1.02±0.03
23	V	37.9 ±0.6	8278	75	1.085±0.010	1.00±0.01	17.9 ±0.3	19.0 ±0.5	150±1	1.08±0.03
25	Mn	41.8 ±0.6	7913	22	1.095±0.010	1.00±0.01	15.4 ±0.3	16.3 ±0.4	147±1	1.05±0.03
26	Fe	49.7 ±0.7	8081	30	1.113±0.015	1.00±0.01	13.5 ±0.3	14.3 ±0.4	146±1	1.10±0.03
26	Fe[c]	49.7 ±0.7	6345	50	1.113±0.015	1.04±0.01	14.4 ±0.3	15.3 ±0.4	153±1	1.12±0.03
27	Co[d]	58.5 ±0.8	8222	60	1.127±0.015	1.00±0.01	10.5 ±0.2	11.2 ±0.3	130±1	1.13±0.04
28	Ni	64.9 ±1.0	7910	50	1.151±0.015	1.00±0.01	7.66±0.2	8.12±0.3	111±1	1.07±0.04
30	Zn	62.1 ±1.0	9195	31	1.143±0.015	1.04±0.01	9.71±0.2	10.3 ±0.3	152±1	0.95±0.03
53	I	117.4 ±3.5	6624	19	1.289±0.030	1.00±0.01	2.78±0.1	2.95±0.1	119±1	0.66±0.07
82	Pb	121.9 ±4.0[e]	3676	18	1.290±0.030	1.04±0.01	1.48±0.05	1.57±0.06	109±1	0.40±0.10

[a] All y_e^- except y_e^- for C, corrected by $f_a = 1.06 \pm 0.02$.
[b] N_e^+ was 3×10^4 for all targets.
[c] Stainless steel.
[d] Λ_t measured in this experiment.
[e] Combined value from J. C. Sens and this experiment.

experimentally impractical. Over the target volume the field compensation was better than 0.05 gauss. A correction by the factor $f_a=1.04$ was made for all e^- yields from all nonferromagnetic targets composed of spin zero nuclei, e.g., C, Ca, Zn, and Pb. The uncertainty of 0.01 is assigned to this particular correction.

3. *Electron and Pion Contamination in the "Muon" Beam*

This factor leads to an uncertainty in the observed number of muon stops in the target. A 10% e^- contamination of the "muon" beam was estimated to affect the observed y^- by 3–5% in the sense of making the apparent yield smaller. With the pure beams used here there is only a negligible correction for this effect.

4. *Anticoincidence Loss*

As mentioned in Sec. IIB, a certain number of the electrons emitted near $t=0$ is suppressed by the action of counter 4 in the telescope ($\bar{4}567$). The anticoincidence delay curve $F(t,T)$ of this combination had a half-width $T=10$ mμsec, leading to losses of the order of 30% for the fastest disappearance rates. The necessary anticoincidence loss correction factor f_{a-c} was computed numerically for each $\Lambda_t(Z)$ as

$$f_{a-c}=\Lambda_t(Z)\int_0^\infty F(t,T)\exp(-\Lambda_t t)dt. \qquad (9)$$

As $F(t,T)$ was known from measurement to better than 10%, the uncertainty in f_{a-c} introduces an error in y^- that does not exceed $\pm 1\%$ for the light and $\pm 3\%$ for the heavy elements.

5. *Total Disappearance Rates*

As mentioned in Sec. IIA, the ultimate limitation on the accuracy with which $R(Z)$ can be determined is set by the uncertainties in the $\Lambda_t(Z)$. For most of the elements measured, $\Lambda_t(Z)$'s were available from the measurements of Sens,[2] or in some cases (Fe, Pb, Co), are weighted mean values of Sens' results and the results of this experiment [method (b) gives $\Lambda_t(Z)$ as a by-product]. The uncertainties in $\Lambda_t(Z)$ are listed in Tables II and III and do not exceed $\sim 1\%$ for low Z elements and $\sim 3\%$ for the high Z elements.

6. *Statistical Uncertainties*

The statistics in the accumulated number of electrons listed in Tables II and III for methods (a) and (b), respectively, contribute to the quoted error in $R(Z)$. These were estimated in the standard fashion.

We now come to the one systematic uncertainty whose importance could not be assumed quantitatively with the techniques used in this experiment. It arises from the following.

7. *Spectral Differences*

While free μ^- mesons should give the same decay spectrum as μ^+ mesons, one would expect the decay spectra of *bound* μ^- mesons to reflect the kinematics of the orbital motion and the influences of the Coulomb field on the outgoing e^-. Some estimates of this spectral "distortion" have appeared in the literature[5,7]; although they are not reliable, they suggest that the effect is not unimportant for medium Z and that it increases with Z. The question arises to what extent the efficiency of our electron telescope reflects, in the comparison of y^- and y^+, from thick targets, these spectral differences. A similar difference in efficiencies may of course also arise when one compares e^- yields from weakly and strongly bound muons (e.g., in the "sandwich" method). As far as the y^-, y^+ comparison is concerned, we have attempted to estimate the necessary corrections both empirically and by a Monte Carlo calculation. Empirically, the absorption of the decay electrons was investigated for (1) $\mu^\pm$ stopping in C, (2) $\mu^\pm$ stopping in Fe. Absorption curves were taken by varying the thickness of the Al absorber (from $\frac{1}{4}$ in. to 1 in. in $\frac{1}{8}$-in. steps) in a slightly modified version of our usual electron telescope. The two curves obtained with C showed no significant difference to within the 1.5% accuracy of the comparison. On the other hand, the Fe absorption curves showed an effect which, extrapolated to zero absorber thickness, corresponds to a $(6.0\pm 1.5)\%$ higher efficiency for counting e^+ than e^-. Thus even with the thick targets used (1 cm of Fe), the anticipated distortion appears to be of consequence. On the bases of these auxiliary experiments we concluded that a factor $f_{sp}=1.06\pm 0.02$ should be applied to the $y^-(Z)$ for the elements near Fe in the periodic table. A crude Monte Carlo calculation (in which a particular e^--spectrum had to be assumed) gave also a correction factor of this magnitude.

There remains a question as to how large a correction factor should be applied to the y^- from the heavy elements I, W, and Pb. Since targets of several radiation lengths thickness were used for these elements, one might agree that the large degradation of the initially different spectra should tend to smear these out and to equalize the differences in the detection efficiencies. The results of some auxiliary y^- measurements performed with Pb targets of varying thickness (i.e., using the target as an absorber) tend to bear out this conjecture. These measurements gave 0.95 ± 0.10 for the ratio, y^+/y^- thus implying that to 10% accuracy this is an effect in Pb. Unfortunately, the low e^- yield from thin Pb targets made a better investigation of this effect impractical.

IV. DISCUSSION OF RESULTS

Figure 6 illustrates the dependence of the bound decay rates $\Lambda_d(Z)$ on Z found in the present experiment as a plot of $R(Z)=\Lambda_d(Z)/\Lambda_d(0)$ *versus* the logarithm

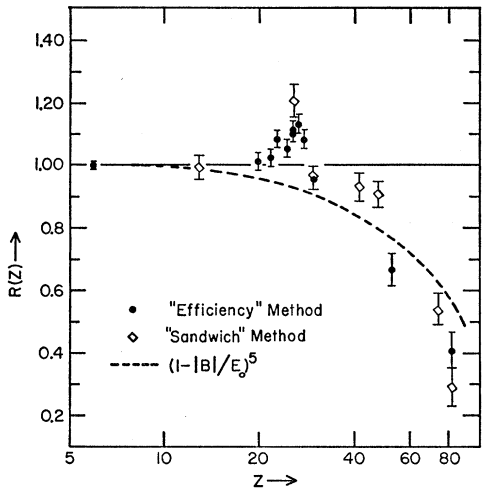

FIG. 6. Plot of $R(Z)=\Lambda_d(Z)/\Lambda_d(0)$ *versus* Z. Experimental values for both Methods (a) and (b) (see text) are indicated. The indicated errors represent the total estimated uncertainties (see Tables II and III). The dashed curve represents the effect of phase space reduction on the decay rate of bound μ^- mesons, neglecting other effects.

of Z. An obvious subdivision of the Z range covered suggests itself: (1) $Z<20$, (2) $20\leq Z\leq 30$, and (3) $Z>30$. In range (1), the decay rate is within the errors of the measurement unaffected by binding (as one would anticipate qualitatively). In range (2), $R(Z)$ exhibits a sharp peak (near Fe, $Z=26$) and is moreover greater than unity, i.e., muons bound to nuclei in this range decay *faster* than they would in vacuo. Finally, in range (3) the decay appears to be greatly slowed down by the binding, being reduced by about a factor 2 in the case of heaviest elements investigated, viz., W and Pb.

As mentioned in the Introduction, there exist as yet no theoretical calculations of $\Lambda_d(Z)$ which would adequately take into account all the obvious features of the bound μ^- decay, and with which one could compare our experimental results. We shall therefore confine ourselves to a comparison with predictions based on a greatly simplified approach, namely one in which only the effect of phase space reduction is accounted for. As $\Lambda_c(0)\sim E_0^5$ (where E_0=muon rest mass),[24] one anticipates $\Lambda_c(Z)\sim(E_0-|B|)^5$, where $B=B(Z)$ is the binding energy of the μ^- in its K orbit. Hence this effect leads to

$$R(Z)=(1-|B|/E_0)^5. \tag{10}$$

The dashed curve in Fig. 6 represents the $R(Z)$ values calculated from relation (10), using *empirical* values[2] of $B(Z)$. These were obtained from the observed mesic $2p-1s$ transition energies by assuming that the $n=2$ terms are not appreciably shifted with respect to their values in the field of point-like nucleus.[25]

While the dashed curve in Fig. 6 [expression (10)] reproduces fairly well the general trend of $R(Z)$, it fails entirely to account for the observed behavior in range (2), both as far as the magnitude (>1) and the Z-dependence of $R(Z)$ are concerned. On purely experimental grounds, the data in this range (2) do not appear to be open to much doubt in either sense. The most striking point, $R(26)$, is supplied by three independent measurements (two by the "efficiency" method and one by the "sandwich" method) which give a weighted mean $R(26)=1.15\pm0.02$. This value is well-supported by an independent (cosmic ray) result of Holstrom and Keuffel[8] who report $R(26)=1.19\pm0.10$. The peak near $Z=26$ is mostly contributed by the ferromagnetic elements Fe, Co, and Ni, and one might raise the question whether the singular behavior displayed by these targets as far as $R(Z)$ is concerned is connected with their magnetic properties, in the sense that the internal magnetic fields could conceivably affect (perhaps differently for μ^+ and μ^-) the remanent polarization of the muons. This possibility appears however ruled out on empirical grounds. As can be seen from Table III, a ferromagnetic Fe target and nonferromagnetic stainless steel target yielded the same results for R. In the latter target, μ^+ mesons exhibited normal precession, i.e., with $\bar{a}=0.22$ and a frequency corresponding to the external field. Furthermore, the nonferromagnetic element V also contributes a point to Fig. 6 which is three standard deviations *above* the $R=1$ line.

It should be noted that the rapid variation of $R(Z)$ for $20\leq Z\leq 30$ is perhaps even more reliably established by experiment than the absolute magnitude of the $R(Z)$'s in this region. Inasmuch as these targets were chosen to have nearly identical radiative properties (see Sec. IIIB), a direct comparison of the $y^-(Z)$'s—without e^+-calibration—can already supply the Z-dependence of R, making the plausible assumption that the e^--spectra do not vary greatly when Z changes by a few units.

Turning now to region (3), one notices that the experimental points for Pb ($Z=82$) lie considerably below the dashed "theoretical" curve (the mean of the two values obtained by the methods quoted being $R(82)=0.34\pm0.03$).

The causes of the observed departures in both regions (2) and (3) from the "theoretical" curve must clearly be sought in effects other than the reduction of the available phase space by binding—i.e., in the effects referred to as (b) and (c) in the Introduction. Effect (b), the influence of the Doppler broadening on the decay spectrum and hence on $\Lambda_d(Z)$ has been included in a crude calculation by Primakoff.[7] In this calculation, which is meant to be applicable only to the heaviest

[24] See, e.g., E. Fermi, *Elementary Particles* (Yale University Press, New Haven, 1951), p. 46.

[25] This procedure appears more appropriate than the one used by Holmstrom and Keuffel (reference 8) who compare their results to the formula $R(Z)=1-5.15(\alpha Z)^2$ due to Khuri (reference 6) and insert for Z the Z_{eff} values used in another context by Wheeler. Khuri's formula appears to be an expansion in (αZ) for *low* values of this parameter.

elements, the state of the μ^- before decay is approximated by a simple harmonic oscillator wave function (as would be correct in the case of an infinitely large nucleus), the mean square displacement being adjusted to give the observed binding energy. This approach gives

$$R(Z)=(1-|B|/E_0)^5F(x), \tag{11}$$

where[26]

$$F(x)=\left\{\left[1-\frac{15}{14x^2}\left(2-\frac{3}{2x^2}\right)\right]P(x) - \frac{45}{14x^3}\pi^{\frac{1}{2}}\exp(-x^2)\right\}, \tag{12}$$

with

$$x=\zeta E_0(1-|B|/E_0)[(\hbar^2/E_0e^2Z)/\zeta]^{\frac{1}{2}},$$

and

$$P(x)=2\pi^{-\frac{1}{2}}\int_0^x \exp(-y^2)dy,$$

ζ being the nuclear "radius." The factor $F(x)$ in Eq. (11) represents the correction for the Doppler broadening and recoil effects neglected in Eq. (10). In evaluating it numerically, we chose $\zeta=7.2\times10^{-13}$ cm, a value which approximates well the exact numerical results of Hill and Ford for Pb. With this choice, Eq. (11) yields $R(82)=0.30$; the inclusion of effects (b) appears thus to improve the agreement with experiment for high Z nuclei.

$R(Z)$ computed according to Eq. (10) or (11) is always less than unity, i.e., both effects (a) and (b) included in its derivation tend to *inhibit* the decay of bound muons. It is hence natural to attribute the behavior observed in range (2), viz., a *stimulation* of the decay,[27] to effects neglected so far, that is either to the effect (c) of the Coulomb field on the outgoing decay electron, or to other unspecified causes. In conjecturing on the effect of the Coulomb field,[28] one should recall that the transition amplitude for any Fermi process is proportional to the product of the wave functions of the four participating fermions taken at the same space-time point. The amplitude of the outgoing e^--wave at the decay point (the μ^- orbit) is expected to increase—with respect to its plane wave value—through the attractive action of the nucleus. Thus this Coulomb effect will tend to *speed up* the bound decays with respect to the vacuum rate $\Lambda_d(0)$. The situation is physically entirely analogous to that encountered in nuclear β^- decay, where a well-known function $f(Z,W_0)$ gives a quantitative measure of the Coulomb enhancement. Tables of this function[29] show that this enhancement does not tend to zero as the available energy W_0 tends to infinity, but rather approaches a constant value. These tables are however not applicable to bound μ^- decay, where (disregarding many other obvious differences) the e^- wave function may go through several oscillations over the region of decay (the volume of the μ^- orbit).

The peak observed in region (2) could thus perhaps be attributed to a competition between the inhibiting effects (a) and (b) and the Coulomb enhancement just discussed. This hypothesis may however have flaws: (1) One would expect the Coulomb enhancement to vary slowly and monotonically as a function of Z, whereas the observed peak around $Z=26$ is a fairly sharp one; (2) The low experimental $R(Z)$ values found for the heaviest elements, reasonably well accounted for by Eq. (10) which neglects the Coulomb enhancement, may become difficult to explain once the latter effect is properly included.

In conclusion, our results can be understood qualitatively on the basis of simple physical arguments without calling for any striking ad hoc hypotheses. Their quantitative comparison with theory is another matter. Since the interaction causing muon decay is by now well understood,[30] an exact and unique theory of bound μ^- decay rates should be essentially a matter of computation. In view of the importance of the finite size of the nucleus in this problem (for both the initial muon and the final electron wave functions), such a computation will however presumably have to be performed numerically for each Z of interest. An effort in this direction has recently been undertaken by Dalitz and Huff,[31] but no results are as yet available for comparison with experiment.

V. ACKNOWLEDGMENTS

I am very grateful to Professor V. L. Telegdi for suggesting this experiment and for his constant guidance and invaluable help during the course of this research. I also wish to express my gratitude to the excellent group of collaborators, R. A. Lundy, R. A. Swanson and J. C. Sens for their help in preparation and performance of this experiment. It is a pleasure to thank Professor H. Primakoff for many stimulating discussions and much useful correspondence.

[26] We thank R. H. Pratt for deriving this expression from H. Primakoff's integral formula.

[27] This expression is used here in the literal sense. In the older literature the term "stimulated decay" was frequently applied to what is now customarily called "muon capture."

[28] Professor V. L. Telegdi was first to point out these Coulomb effects on the outgoing electron wave function to us.

[29] See, e.g., K. Siegbahn, *Beta- and Gamma-Ray Spectroscopy* (Interscience Publishers, New York, 1955).

[30] Gatlinburg Conference on Weak Interactions, October, 1958. [Bull. Am. Phys. Soc. 4, 76–84 (1959).]

[31] Dalitz and Huff (private communication).